Monolithic nanoporous copper fabricated through decomposition and sintering of oxalate

Bing Li, Mingyu Li ✉, *Qingxuan Zeng, Xingyu Wu*

State Key Laboratory of Explosion and Technology, Beijing Institute of Technology, Beijing 100081, People's Republic of China
✉ *E-mail: mingyuli@163.com*

Published in Micro & Nano Letters; Received on 18th February 2016; Revised on 13th April 2016; Accepted on 13th April 2016

Two more simple methods were used for preparation of the monolithic nanoporous copper. One was that through decomposition and sintering of copper oxalate precipitate directly. The other was that through decomposition and sintering of copper oxalate and manganese oxalate. The effects of sintered temperature and holding time on the morphology of the monolithic nanoporous copper were investigated. Thermal decomposition, composition and morphology of copper oxalate precipitate, as well as microscopic morphology and specific surface area of the monolithic nanoporous copper were analysed by thermogravimetric analysis, X-ray diffraction, scanning electron microscope and nitrogen adsorption–desorption. The preferable nanoporous copper can be prepared by decomposition and sintering of copper oxalate directly at 400°C for 30 min. The prepared monolithic nanoporous copper is of open and interconnected pores and is made up of copper grains with the size of about 100 nm, which is as high as 69.9 $m^2 g^{-1}$ in specific surface area.

1. Introduction: Recently, scholars have paid great attention to the combination of micro-electromechanical systems (MEMS) and fuze with the continuous development of MEMS. MEMS fuze is of smart, intelligent, miniaturised features [1]. With in-depth development of the MEMS fuze, traditional charge technology cannot fulfil the requirements of miniaturisation, therefore new micro-charge technology has become essential. It is reported [2, 3] that nanoporous copper can be used as the precursor of explosive. Specifically, the monolithic nanoporous copper was pressed into a polycarbonate confinement and then reacted with the gaseous azoimide to generate copper azide by 'in-situ' method. This technology avoided the direct handling of the sensitive primary explosive. A miniature device for shock initiation of hexanitrostilbene by micro-charge detonation-driven flyer was fabricated. The HNS-IV explosive with density 1.57 g cm^{-3} was initiated successfully by such miniature device. More attention should be paid that the mass of micro-charge under the preferable conditions is <0.7 mg [4]. Moreover, it removes the necessity for handling, loading, transportation and storage of bulk quantities of sensitive primary explosive and therefore largely improves the safety of fabrication. Furthermore, it can be combined with the MEMS safety-and-arming devices, which will largely improve the safety of usage. It can be predicted that such initiation device will have a tremendous prospect for the practical applications.

Nanoporous metal often displays novel physical, chemical and mechanical properties due to its high specific surface area, low density and interconnected pore. These properties show promise for a variety of scientific and engineering applications, including catalysis [5], filter [6], sensor [7], surface-enhanced Raman spectroscopy [8] and so forth. Preparation of nanoporous copper primarily involves the means of dealloying [9–13], colloidal crystal template [14, 15] and hydrogen bubble template [16–21]. Currently, dealloying, a selective dissolution of more active component of an alloy, has been reported to be a simple approach to fabricate monolithic nanoporous metal [22, 23]. However, it is not easy to dissolve the more active metal of alloy thoroughly, especially when increasing the thickness of alloy.

Copper oxalate is a material with an unusual antiferromagnetic characteristic, which can be used as a precursor for preparation of copper nanoparticles by thermal decomposition in the absence of oxygen [24, 25]. In this work, we develop two more simple synthesis routes for preparing monolithic nanoporous copper. One is that by decomposition and sintering of copper oxalate directly. The other is that by decomposition and sintering of copper oxalate and manganese oxalate prepared by coprecipitation method and then dissolving the part of manganese in a 1 M HCl solution.

2. Experimental

2.1 Sample preparation: Copper oxalate precipitate was synthesised according to this procedure: the copper nitrate (0.015 mol) was dissolved into 25 ml of anhydrous alcohol to form a homogeneous solution. An amount of oxalic acid (molar ratio of 2:1 relative to copper nitrate) dissolved in 20 ml of anhydrous alcohol was quickly added into the above solution under magnetic stirring intensely. The solution was stirred for about 60 min. The product was dried at 130°C for overnight.

The preparation of copper oxalate and manganese had a similar process. The copper nitrate (0.01 mol) and the manganese oxalate (0.005 mol) were dissolved into 25 ml of anhydrous alcohol to form a homogeneous solution. The oxalic acid (0.03 mol) dissolved in 20 ml of anhydrous alcohol was quickly added into the above solution under magnetic stirring intensely. The solution was stirred for about 60 min. The product was dried at 90°C for overnight.

The dried copper oxalate precipitate was grinded and compacted with the pressure of 10 MPa, leading to the product of green sample. The green sample was subsequently heated under controlled temperature to decompose the copper oxalate precipitate completely and finally sintered in a tube furnace in nitrogen (N_2) environment. This is named as low-temperature decomposing process and high-temperature sintering process, respectively. The CO_2 gas was generated in the decomposing process of copper oxalate, which played the role of the pore-forming agent. Similarly, the dried copper oxalate and manganese oxalate coprecipitate was grinded and compacted with the pressure of 10 MPa, leading to the product of green sample. The green sample was subsequently heated under controlled temperature to decompose the copper oxalate and manganese oxalate coprecipitate completely and finally sintered in a tube furnace in N_2 environment. Then, the product was dissolved in a 1 mol l^{-1} HCl solution for

doi: 10.1049/mnl.2016.0034

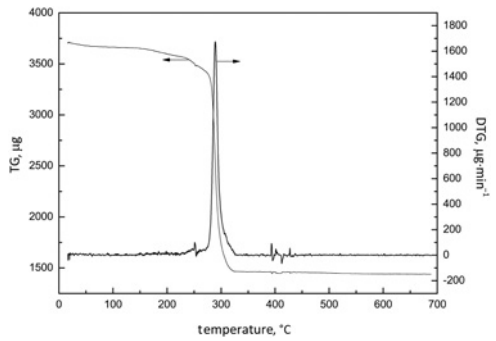

Fig. 1 *TG-DTA of the copper oxalate precipitate*

1 h. The sample was rinsed with distilled water and anhydrous alcohol, and kept in a vacuum chamber to avoid oxidation.

2.2 Characterisation: Morphology of all synthesised samples was characterised by scanning electron microscopy (SEM). Scanning electron microscopic images were recorded by a Hitachi S-4700 series instrument equipped with an energy-dispersive X-ray spectroscopy. The samples were sputtered with gold before examination. X-ray powder diffraction (XRD) patterns were recorded by a Germany Bruker D8-Advance X-ray diffractometer using Ni-filtered Cu-Kα radiation. Thermogravimetric-differential thermal analysis (TG-DTA) was carried out using a thermal gravimetric analysis instrument (SII TG/DTA 6300) with the flow of N_2 and a heating rate of 10°C min^{-1}. To evaluate the specific surface areas of these as-prepared samples, the N_2 adsorption/desorption experiments were carried out on a Nova Station automatic surface area and pore radius distribution apparatus (Nove 2200e).

3. Results and discussion: The TG-DTA curve of the copper oxalate precipitate is shown in Fig. 1. As shown in Fig. 1, a small amount of weight loss appears before 250°C, which may be due to the evaporation of trace amount of moisture, coupled with the decomposition of excess oxalic acid in the copper oxalate precipitate. There is only one weight loss step in the temperature range from 250 to 320°C. The weight loss at 250–320°C may be ascribed to the decomposition of the copper oxalate. The weight loss is about 58%, which is close to the theoretical value of the copper oxalate without crystal water. In the experiment, finally sintering process was heated at 320°C for 60 min and sintered at 400–500°C at intervals of 50°C for different holding time (30, 60 and 120 min) with both heating rate and cooling rate being set at 3°C min^{-1}. It should be pointed out that the heating rate and the cooling rate must be kept at a low level to avoid cracking of the samples during the decomposing process and the cooling process, due to the release of CO_2 gas and the thermal stress.

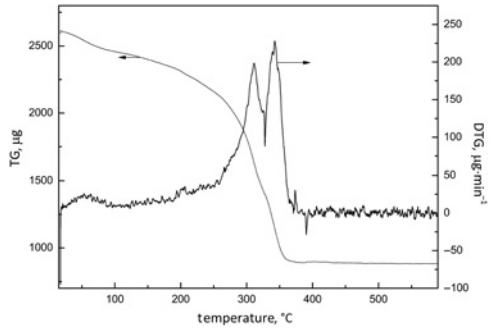

Fig. 2 *TG-DTA of the copper oxalate and manganese oxalate coprecipitate*

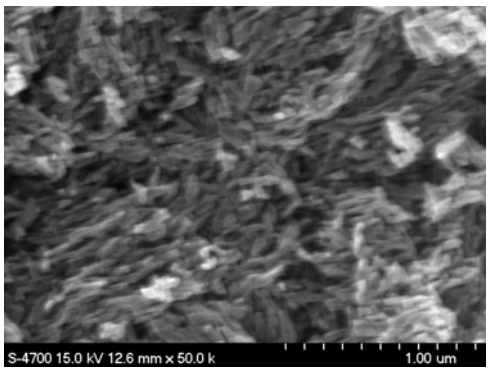

Fig. 3 *SEM image of the copper oxalate precipitate*

Fig. 2 shows the TG-DTA curve of the copper oxalate and manganese oxalate coprecipitate. As shown in Fig. 2, there is scarcely any weight loss when the temperature exceeds 360°C. There are two weight loss steps in the temperature range from 250 to 350°C, which can be attributed to the decomposition of copper oxalate and manganese oxalate, respectively. Thus, finally sintering process was heated at 360°C for 30 min and sintered at 500–700°C at intervals of 100°C for 60 min with both heating rate and cooling rate being set at 3°C min^{-1}.

Fig. 3 shows the SEM image of the copper oxalate precipitate. As can be seen from the micrograph in Fig. 3, the precipitate is composed of particles of like-flocculent, which is different from the results reported in the vast majority of literature. In addition, the agglomeration phenomenon of particles is very obvious. These may be attributed to the absence of filtering and washing towards the precursor solution. As presented in Fig. 3, the mean diameter of particles is <100 nm.

Fig. 4 (a) shows XRD pattern of particles shown in Fig. 3, which indicates their crystalline nature. Location of the major peaks clearly verified composition of this material to be mainly copper oxalate. As can be seen in Fig. 4 (a), there are still some weak peaks of impurities presented in the spectrum, which is possibly attributed to the absence of filtering and washing towards precursor solution likewise. The mean crystallite size of the copper oxalate precipitate is ∼21 nm, estimated from the half-width of (100) peak using Scherrer equation. XRD pattern of nanoporous copper obtained through decomposition and sintering of the copper oxalate precipitate is shown in Fig. 4 (b). The XRD pattern is consistent with the spectrum of copper, and no peak attributable to possible impurities is observed. It implies that the impurities

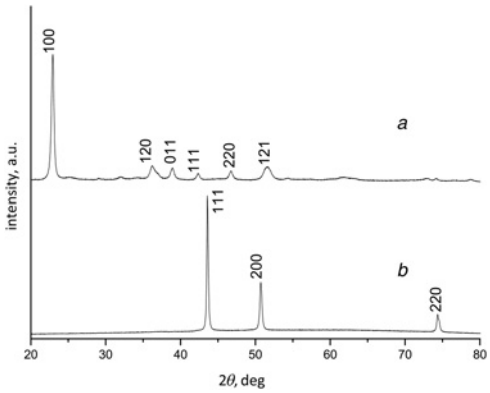

Fig. 4 *XRD pattern of the copper oxalate precipitate and the synthesised nanoporous copper (a), the copper oxalate precipitate and (b) synthesised nanoporous copper through decomposition and sintering of copper oxalate precipitate at 400°C for 30 min*

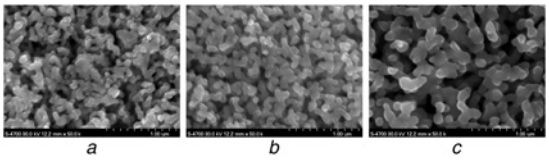

Fig. 5 *SEM images of nanoporous copper obtained through decomposition and sintering of copper oxalate precipitate with holding time for 30 min and sintering at*
a 400°C
b 450°C
c 500°C

inside the copper oxalate precipitate can be eliminated thoroughly via calcination. This pattern for XRD spectrum of the sample indicates that nanoporous copper synthesised by calcination of the copper oxalate precipitate has a high crystallinity and purity. Estimated from Scherrer equation, the average crystallite size of the prepared nanoporous copper is about 38 nm.

3.1 Effect of sintering temperature on morphology of monolithic nanoporous copper: Sintering temperature must be selected by considering the material, the powder shape and the powder particle size. Finer powder particles require a lower sintering temperature since the surface energy driving force to initiate bond growth is much higher than for a coarser particle. Thence, sintering temperature is extremely critical to fabricate nanoporous copper by the decomposition and sintering of the copper oxalate precipitate and the copper oxalate and manganese oxalate coprecipitate.

Fig. 5 shows the typical SEM images of as-synthesised samples obtained through decomposition and sintering of the copper oxalate precipitate with the holding time for 30 min and sintering at different temperature. When the sintering temperature reaches 400°C, a uniform porous structure with length scales of ~100 nm can be obtained in the as-synthesised samples (Fig. 5*a*). Meanwhile, an open and interconnected pore structure can be observed.

With the sintering temperature up to 450°C, the sample surface exhibits a porous structure with length scales of 150–200 nm and an open, bicontinuous interpenetrating ligament-pore structure. As to the nanoporous copper upon sintering at 500°C, its microstructure can be characterised by a three-dimensional bicontinuous network morphology with dramatically larger ligament sizes of 200–300 nm as compared with that of nanoporous copper sintering at 400 and 450°C. In addition, the pore size of nanoporous copper sintering at 500°C is also larger than that of nanoporous copper sintering at 400 and 450°C.

Fig. 6 shows the typical SEM images of as-synthesised samples obtained through decomposition and sintering of the copper oxalate and manganese oxalate coprecipitate under the condition of holding time for 60 min and sintering at different temperature. When the sintering temperature reaches 500°C, a uniform porous structure with length scales of ~200 nm can be obtained in the as-synthesised samples (Fig. 6*a*).

Meanwhile, an open and interconnected pore structure can be observed. With the sintering temperature up to 600°C, the sample

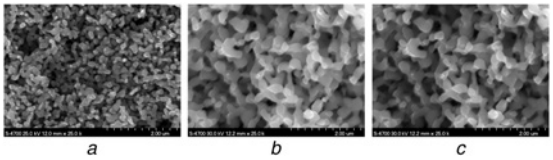

Fig. 6 *SEM images of nanoporous copper obtained through decomposition and sintering of copper oxalate and manganese oxalate coprecipitate with holding time for 60 min and sintering at*
a 500°C
b 600°C
c 700°C

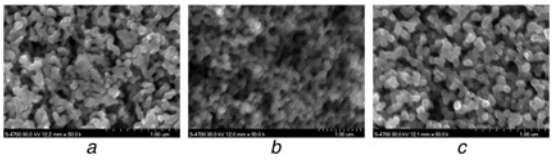

Fig. 7 *SEM images of nanoporous copper obtained through decomposition and sintering of copper oxalate precipitate with sintering temperature at 400°C and holding time for*
a 60 min
b 80 min
c 120 min

surface exhibits a porous structure with length scales of 300–400 nm and an open, bicontinuous interpenetrating ligament-pore structure. When the sintering temperature reaches 700°C, the pore of sample reduces significantly, and the sample reveals a more dense morphology.

3.2 Effect of holding time on morphology of monolithic nanoporous copper: The sintering time is also known as the holding time, which must be monitored to allow for a minimum exposure time at the desired sintering temperature. Sintering for at least 60 min at the maximum sintering temperature is recommended for most materials for sufficient bond formation and growth. Inadequate sintering time can lead to tremendous variations in part shrinkage and final density causing porosity and permeability variations. Sufficient holding time is also very significant to prepare nanoporous copper.

Fig. 7 shows the typical SEM images of as-synthesised samples obtained through decomposition and sintering of the copper oxalate precipitate under the condition of sintering temperature at 400°C and different holding time. As shown in Fig. 7, the impact of holding time on the shape of ligament particle is more apparent than on the size of ligament. When the holding time is 60 min, the ligament particle shows the shape of columnar, compared with the globose particle when the holding time is 80 and 120 min. However, with the increase in holding time, the size of ligament particle slightly grows. Meanwhile, the size of pore gradually decreases with the increase in holding time.

The specific surface areas of the porous samples can be evaluated based on N_2 adsorption/desorption experiments. Figs. 8 and 9 show the N_2 adsorption/desorption isotherm for monolithic nanoporous copper fabricated through decomposition and sintering of the copper oxalate precipitate at 400°C for 30 min and through decomposition and sintering of the copper oxalate and manganese oxalate coprecipitate at 500°C for 60 min, respectively. The result shows

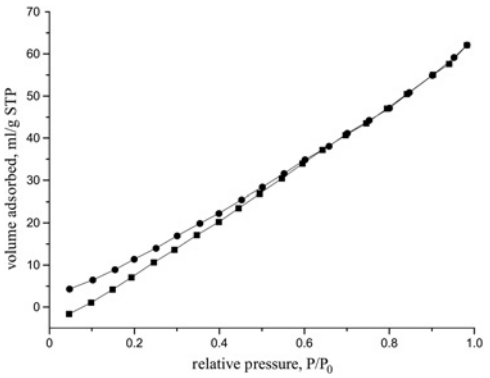

Fig. 8 *N_2 isotherm at 77 K for monolithic nanoporous copper fabricated through decomposition and sintering of copper oxalate precipitate at 400°C for 60 min [$S_{BET} = V_m \cdot N \cdot \sigma_m$, where V_m is the saturated adsorbed volume for monomolecular layer, N is the Avogadro constant (6.023×10^{23} mol^{-1}) and σ_m is the cross-sectional area for N_2 molecule (0.162 nm^2)]*

doi: 10.1049/mnl.2016.0034

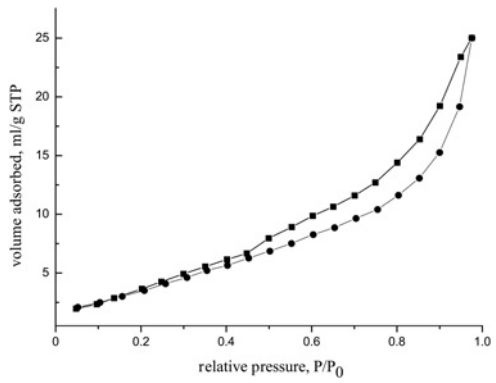

Fig. 9 *N_2 isotherm at 77 K for monolithic nanoporous copper fabricated through decomposition and sintering of the copper oxalate and manganese oxalate coprecipitate at 500°C for 60 min [$S_{BET} = V_m \cdot N \cdot \sigma_m$, where V_m is the saturated adsorbed volume for monomolecular layer, N is the Avogadro constant (6.023×10^{23} mol^{-1}) and σ_m is the cross-sectional area for N_2 molecule (0.162 nm^2)]*

that the Brunauer–Emmett–Teller (BET) surface area of the monolithic nanoporous copper through decomposition and sintering of the copper oxalate precipitate at 400°C for 30 min is much high and has been determined to be 69.9 m^2 g^{-1}. The BET surface area of the monolithic nanoporous copper through decomposition and sintering of the copper oxalate and manganese oxalate coprecipitate at 500°C for 60 min has been determined to just be 7.1 m^2 g^{-1}. Besides, with the sintering temperature and holding time increasing, the specific surface areas of the samples decrease sharply. This phenomenon may be well attributed to the reducing and even disappearing of the small pore between the particles, coupled with the growth of copper particles. It is worthwhile noting that this interesting structural feature endows the nanoporous copper with higher surface area, which indicates the fabricated nanoporous copper with upper reactivity morphology.

4. Conclusions: In summary, we develop two new synthesis routes for preparing monolithic nanoporous copper, which includes the decomposition and sintering of the copper oxalate precipitate and the decomposition and sintering of the copper oxalate and manganese oxalate coprecipitate in an inert atmosphere. The copper oxalate precipitate is composed of particles of like-flocculent, and the average size of particles is <100 nm. The sintering temperature and the holding time have significant effect on the morphology of nanoporous copper. With increasing the sintering temperature, the size of ligament particle gradually increases and the size of pore decreases. In addition, the specific surface areas sharply decrease with increasing the sintering temperature. When increasing the holding time, the shape of ligament particle becomes spherical while the size of particle is almost unchanged. The porosity of nanoporous copper depends mainly on the sintering temperature and holding time by decomposition and sintering of copper oxalate, while it depends primarily on the proportion of manganese oxalate by decomposition and sintering of copper oxalate and manganese oxalate. Therefore, the nanoporous copper possesses larger pore size and wider variation for porosity fabricated by the latter method. However, the latter method needs higher sintering temperature, which leads to lager particle size and lower specific surface area. The ligaments and nanopore channels of nanoporous copper formed by sintering at 400°C and holding time for 60 min are more uniform than that of under other conditions. Under this condition, the prepared monolithic nanoporous copper is of a uniform sponge-like morphology with an average ligament diameter of 100 nm.

5. Acknowledgments: This work was supported by the Project of State Key Laboratory of Explosion Science and Technology, P. R. China (YBKT13-03 and YBKT12-03), and Specialized Research Fund for the Doctoral Program of Higher Education of China (20131101110009).

6 References

[1] Niu L., Shi K., Zhao X., *ET AL.*: 'Application of MEMS on fuses', *Chin. J. Detect. Control*, 2008, **30**, (6), pp. 54–59
[2] Jean D.: 'MEMS micro-detonator based fuzing'. The 53rd Annual Fuze Conf., Orlando, USA, 2009
[3] Toon J.: 'Explosives on a chip: unique porous copper structure enables new generation of military micro-detonators', *Res. Horiz.*, 2007, **25**, (1), pp. 22–23
[4] Zeng Q.X., Jian G.Z., Li B., *ET AL.*: 'The fitted parameters of JWL equation of state for copper azide', *Chin. Initiators Pyrotechnics*, 2014, **6**, pp. 28–31
[5] Dong C., Zhong M., Li L., *ET AL.*: 'Fabrication and functionalization of tunable nanoporous copper structures by hybrid laser deposition and chemical dealloying', *Sci. Adv. Mater.*, 2012, **4**, pp. 204–213
[6] Tang Y., Tang B., Qing J.B., *ET AL.*: 'Nanoporous metallic surface: facile fabrication and enhancement of boiling heat transfer', *Appl. Surf. Sci.*, 2012, **258**, pp. 8747–8751
[7] Bonroy K., Friedt J.M., Frederix F., *ET AL.*: 'Realization and characterization of porous gold for increased protein coverage on acoustic sensors', *Anal. Chem.*, 2004, **76**, pp. 4299–4306
[8] Chen L.Y., Yu J.S., Fujita T., *ET AL.*: 'Nanoporous copper with tunable nanoporosity for SERS applications', *Adv. Funct. Mater.*, 2009, **19**, pp. 1221–1226
[9] Hayes J.R., Hodge A.M., Biener J., *ET AL.*: 'Monolithic nanoporous copper by dealloying Mn–Cu', *J. Mater. Res.*, 2006, **21**, pp. 2611–2616
[10] Jia F., Yu C., Deng K., *ET AL.*: 'Nanoporous metal (Cu, Ag, Au) films with high surface area: general fabrication and preliminary electrochemical performance', *J. Phys. Chem. C*, 2007, **111**, pp. 8424–8431
[11] Lu H.B., Li Y., Wang F.H.: 'Synthesis of porous copper from nanocrystalline two-phase Cu–Zr film by dealloying', *Scr. Mater.*, 2007, **56**, pp. 165–168
[12] Qi Z., Zhao C., Wang X., *ET AL.*: 'Formation and characterization of monolithic nanoporous copper by chemical dealloying of Al–Cu alloys', *J. Phys. Chem. C*, 2009, **113**, pp. 6694–6698
[13] Li M., Zhou Y., Geng H.: 'Fabrication of nanoporous copper ribbons by dealloying of Al–Cu alloys', *J. Porous Mater.*, 2011, **19**, pp. 79–796
[14] Lan D., Wang Y., Ma W., *ET AL.*: 'The key factors in fabrication of high-quality ordered macroporous copper film', *Appl. Surf. Sci.*, 2008, **254**, pp. 6775–6778
[15] Zein El Abedin S., Prowald A., Endres F.: 'Fabrication of highly ordered macroporous copper films using template-assisted electrodeposition in an ionic liquid', *Electrochem. Commun.*, 2012, **18**, pp. 70–73
[16] Shin H.C., Dong J., Liu M.: 'Nanoporous structures prepared by an electrochemical deposition process', *Adv. Mater.*, 2003, **15**, (19), pp. 1610–1614
[17] Shin H.C., Liu M.: 'Copper foam structures with highly porous nanostructured walls', *Chem. Mater.*, 2004, **16**, pp. 5460–5464
[18] Li Y., Jia W.Z., Song Y.Y., *ET AL.*: 'Superhydrophobicity of 3D porous copper films prepared using the hydrogen bubble dynamic template', *Chem. Mater.*, 2007, **19**, pp. 5758–5764
[19] Kim J.H., Kim R.H., Kwon H.S.: 'Preparation of copper foam with 3-dimensionally interconnected spherical pore network by electrodeposition', *Electrochem. Commun.*, 2008, **10**, pp. 1148–1151
[20] Nam D.H., Kim R.H., Han D.W., *ET AL.*: 'Effects of $(NH_4)_2SO_4$ and BTA on the nanostructure of copper foam prepared by electrodeposition', *Electrochim. Acta*, 2011, **56**, pp. 9397–9405
[21] Nikolić N.D., Branković G., Maksimović V.M., *ET AL.*: 'Influence of potential pulse conditions on the formation of honeycomb-like copper electrodes', *J. Electroanal. Chem.*, 2009, **635**, pp. 111–119
[22] Liu W.B., Zhang S.C., Li N., *ET AL.*: 'A general dealloying strategy to nanoporous intermetallics, nanoporous metals with bimodal, and unimodal pore size distributions', *Corros. Sci.*, 2012, **58**, pp. 133–138
[23] Mao R., Liang S., Wang X., *ET AL.*: 'Effect of preparation conditions on morphology and thermal stability of nanoporous copper', *Corros. Sci.*, 2012, **60**, pp. 231–237
[24] Masoud S.N., Davar F., Mir N.: 'Synthesis and characterization of metallic copper nanoparticles via thermal decomposition', *Polyhedron*, 2008, **27**, pp. 3514–3518
[25] Lv J.J., Li M.Y., Zeng Q.X.: 'Preparation and characterization of copper oxide and copper nanoparticles', *Adv. Mater. Res.*, 2011, (308–310), pp. 715–721